

## Chapter 2

# Solid Oxide Fuel Cells

Chendong Zuo, Mingfei Liu and Meilin Liu

**Abstract** Solid oxide fuel cells (SOFCs) have potential to be the most efficient and cost-effective system for direct conversion of a wide variety of fuels to electricity. The performance and durability of SOFCs depend strongly on the microstructure and morphology of cell components. As a unique synthesis and processing technique with easy control of composition, structure, morphology, and microstructure, sol-gel processes have been widely used for fabrication of key SOFC materials or critical components with desired properties or functionalities unattainable otherwise. In this chapter, we provide an overview on sol-gel processes applied for preparation of homogeneous and fine powders of electrolyte, electrode, and ceramic interconnect materials, for deposition of dense electrolyte membranes or porous electrode films, and for modification of electrode or metallic interconnect surface or interface to enhance catalytic activity, to improve tolerance to coking or contaminant poisoning, and to increase stability against oxidation, reduction, or other degradation mechanisms. While significant progress has been made in controlling and tailoring the composition, microstructure, morphology, and hence functionality of materials and components, many challenges still remain to make sol-gel processes cost-effective and versatile for many applications. The development of novel sol-gel processes as well as the exploration of the existing ones to new applications continues to be an intriguing research pursuit.

---

C. Zuo · M. F. Liu · M. L. Liu (✉)  
School of Materials Science and Engineering,  
Center for Innovative Fuel Cell and Battery Technologies,  
Georgia Institute of Technology, 771 Ferst Drive,  
Atlanta, GA 30332-0245, USA  
e-mail: meilin.liu@mse.gatech.edu

C. Zuo  
e-mail: zuochd@hotmail.com

M. F. Liu  
e-mail: mingfei.liu@mse.gatech.edu

**Keywords** Anode • Cathode • Coatings • Electrode/electrolyte interface • Electrolyte • Gadolinia-doped ceria (GDC) • ILTSOFC • Lanthanum strontium manganate (LSM) • Magnesium doped lanthanum chromate • NiO/YSZ • Sol-gel • Solid oxide fuel cell (SOFC) • Surface modification • Yttria-stabilized Zirconia (YSZ)

## 2.1 Introduction

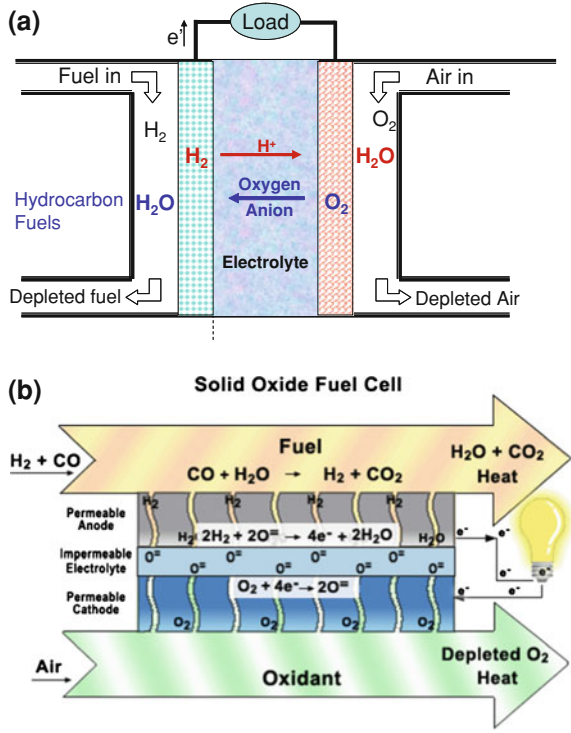
A fuel cell is a system that converts the chemical energy of a fuel directly to electricity. Compared to other types of fuel cells, a solid oxide fuel cell (SOFC) is an all-solid-state fuel cell based on a solid oxide electrolyte [1], which potentially offers the highest energy efficiency with minimum emissions and hold promise for direct utilization of a wide variety of fuels, from hydrogen to natural gas, coal gas, reformed gasoline or diesel, and gasified carbonaceous solids (e.g. municipal solid waste and biomass) [2–4]. SOFCs are simple, reliable, environmentally benign, and highly efficient (up to ~85% energy efficiency when combined with gas turbine) compared to engines and modern thermal power plants (~30%) [5].

### 2.1.1 Configuration of a SOFC

A single SOFC consists of an anode and a cathode separated by a solid oxide electrolyte (an ionic conductor), as schematically shown in Fig. 2.1a [6]. The solid electrolyte can be an *oxygen ion*, a *proton*, or a *mixed oxygen ion–proton* conductor, but it must be an electronic insulator (prohibiting the conduction of electrons or electron holes) and gas impermeable (in a dense membrane form). While SOFCs based on proton conductors (e.g.,  $\text{BaZr}_{0.1}\text{Ce}_{0.7}\text{Y}_{0.2}\text{O}_{3-\delta}$ —based electrolytes) have attracted much attention in recent years, the most studied SOFC systems to date are based on oxygen ion conductors such as yttria-stabilized zirconia electrolyte (YSZ, with a composition of 8 mol.%  $\text{Y}_2\text{O}_3$ –92 mol.%  $\text{ZrO}_2$ , sometimes referred as 8YSZ); the anode is a porous nickel-YSZ cermet; and the cathode is a porous composite that usually contains YSZ and  $\text{La}_{1-x}\text{Sr}_x\text{MnO}_{3-\delta}$  (LSM, usually  $x$  varies from ~0.15 to ~0.20). YSZ-based SOFCs usually operate at high temperatures (750–1,000°C) to be efficient because of the limited transport and catalytic properties of the SOFC materials at low temperatures. To reduce the operating temperature, doped ceria (such as  $\text{Ce}_{0.9}\text{Gd}_{0.1}\text{O}_{2-\delta}$  or GDC and  $\text{Ce}_{0.9}\text{Sm}_{0.1}\text{O}_{2-\delta}$  or SDC) have been used as the electrolyte and  $\text{La}_{0.6}\text{Sr}_{0.4}\text{Co}_{0.2}\text{Fe}_{0.8}\text{O}_{3-\delta}$  (LSCF) as the cathode for SOFCs to be operated at low temperatures (<700°C). Figure 2.1b is a schematic for a typical single SOFC based on an electrolyte of an oxygen ion conductor using hydrogen as the fuel and oxygen as the oxidant.

During operation, oxygen molecules are adsorbed, dissociated, and reduced on the cathode surface to ionic oxygen species before incorporated into the lattice as

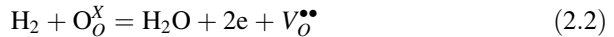
**Fig. 2.1** Schematics of (a) SOFC based on different types of solid electrolyte [6] and (b) operating concept of an SOFC based on an oxygen ion conducting electrolyte [7]



oxygen ions, which then move through the electrolyte to the anode and combine with fuel molecules to form water and carbon monoxide/dioxide (if a hydrocarbon fuel is used). Outside the cell, electrons move from the anode to the cathode through an external circuit, converting chemical energy of the fuel to electrical energy. In Kroger's notation, oxygen reduction on the cathode can be described as follows:



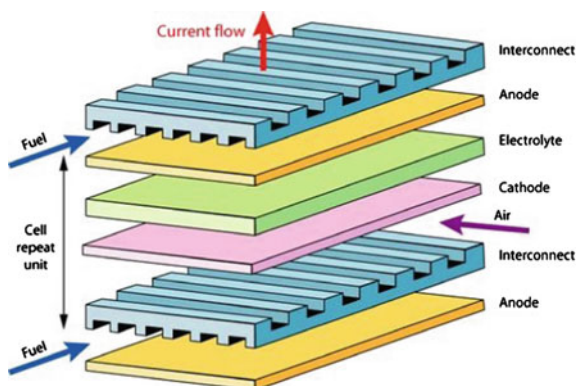
At the same time, fuel molecule (e.g., hydrogen) is oxidized on the anode by combining with oxygen ions and release electrons:



The combination of the reactions (2.1) and (2.2) yields the overall reaction of the fuel cell,



**Fig. 2.2** Schematic for a planar SOFC design [8]



### 2.1.2 Solid Oxide Fuel Cell Structure

For practical applications, SOFCs have different structures, and each of them has its own advantages and disadvantages, though the materials for cell components in these different designs are either the same or very similar in nature.

- Planar versus tubular solid oxide fuel cells

Currently, there are two basic types of SOFCs in terms of cell structure: one is planar and the other is tubular. For planar SOFCs, each cell is made into a flat disk, square, or rectangular plate. The cells are put in series and connected by the interconnect plates, as schematically shown in Fig. 2.2. For tubular SOFCs, usually the electrode (either cathode or anode) is made into a long-tube with a porous wall. Outside the electrode tube are the electrolyte and then another electrode. Cells are also connected in series through interconnects, as schematically shown in Fig. 2.3. Earlier studies in SOFCs were focused on high temperature tubular SOFC systems; since the late 1990s, accompanied with the reduction of electrolyte thickness in the planar SOFC technology, the development of planar SOFC systems has drawn great interest due to its apparent advantages in power density and the ease of fabrication. However, tubular SOFC is still favorable for portable applications where rapid start-up and cool-down are required. The comparisons of planar and tubular structures are summarized in Table 2.1 [1].

- Electrolyte-supported versus electrode-supported solid oxide fuel cells

As illustrated in Fig. 2.1, a single SOFC has three layers: a porous anode and a porous cathode separated by a dense electrolyte membrane. The relative thickness for each cell component depends on the cell structure, electrolyte-supported or electrode-supported SOFCs, as illustrated in Fig. 2.4. In terms of processing technique, electrode-supported cells are more demanding than electrolyte-supported cells. However, electrode-supported structures are now more widely used. For example, for the tubular structure, Siemens adopts the cathode-supported

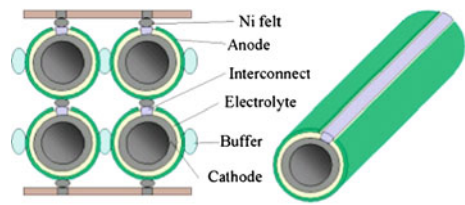


**Fig. 2.3** Schematic for a tubular SOFC design [9]

**Table 2.1** Comparison of planar and tubular structure for solid oxide fuel cells [1]

	Planar	Tubular
Power per unit area	Higher	Lower
Power per unit volume	Higher	Lower
Ease of fabrication	Easier	Difficult
Cost of fabrication	Higher	Lower
Ease of sealing	Difficult	Easy
Long-term stability	Fair	Excellent
Thermo-cycling stability	Fair	Good

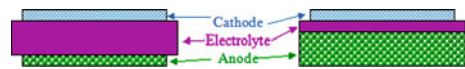


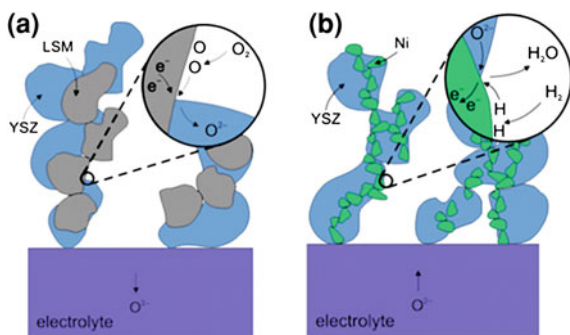
**Fig. 2.4** Schematic for the cross-section of (a) an electrolyte-supported SOFC and (b) an anode supported SOFC

structure, and for the planar structure, most industrial teams adopt the anode-supported structure. The main advantage of the electrode-supported structure is that it provides thinner electrolyte and thus lower electrolyte ohmic resistance, which enables the operation of SOFC at lower temperatures, especially for the anode-supported planar structure [1].

**2.1.3 Advanced Intermediate- and Low-Temperature SOFCs (ILT-SOFCs)**

SOFC is currently attracting tremendous interest because of its huge potential for power generation in stationary, portable, and transport applications and of the increasing need for sustainable energy resources. The major current impediment of commercializing SOFCs is the high cost which results from high operating temperature (800–1,000°C). By lowering the operating temperature (500–750°C), the advanced intermediate- and low-temperature SOFCs (ILT-SOFCs) have the potential to greatly reduce the cost of interconnect, manifolding, and sealing materials, in addition to improved reliability, portability, and operational life [10]. However, the interfacial polarization resistances between electrolyte and

**Fig. 2.5** Schematic of (a) Reduction reaction on the TPB of a cathode made of LSM-YSZ and (b) Oxidation reaction on the TPB of an anode made of Ni-YSZ [13]



electrodes increase dramatically as the operating temperature is reduced [11]. Thus, the development of novel electrode materials and/or unique microstructure is one of the critical issues in development of new generation SOFCs.

As shown in Fig. 2.5, a critical part of most fuel cells is often referred to as the triple-phase boundary (TPB), where the actual electrochemical reactions take place, are found where reactant gas, electrolyte, and electrode meet each other. For a site or area to be active, it must be exposed to the reactant, be in electrical contact with the electrode, be in ionic contact with the electrolyte, and contain sufficient electro-catalyst for the reaction to proceed at a desired rate. The density of these regions and the microstructure of these interfaces play a critical role in the electrochemical performance of SOFCs [12]. Thus porous electrodes with fine particle size are preferred in SOFCs to achieve high surface area which significantly increases the length of TPB. In order to reduce the operating temperature, the resistive loss occurring in the electrolyte should also be minimized. One of the solutions is to decrease the thickness of the solid electrolyte from several hundred micrometers, the usual thickness in conventional electrolyte-supported cell, to a range close to ten micrometers (electrode-supported cell). Therefore, advanced fabrication processes are desirable in order to create dense, thin electrolyte and porous electrode films with fine microstructures so that electrochemical performance can be enhanced at lower operating temperatures.

### 2.1.4 Applications of Sol-Gel Process in SOFCs

Sol-gel processes have been widely used for synthesis of an inorganic network through a chemical reaction in a solution at low temperatures. The most obvious features of this reaction, the transition from a liquid into a solid (di- or multi-phasic gel), led to the expression “sol-gel process” [14]. An overview of the sol-gel process is presented in a simplified chart (Fig. 2.6).

Sol-gel chemistry is a remarkably versatile approach for fabricating materials and components. The advantages of the sol-gel processes include excellent control

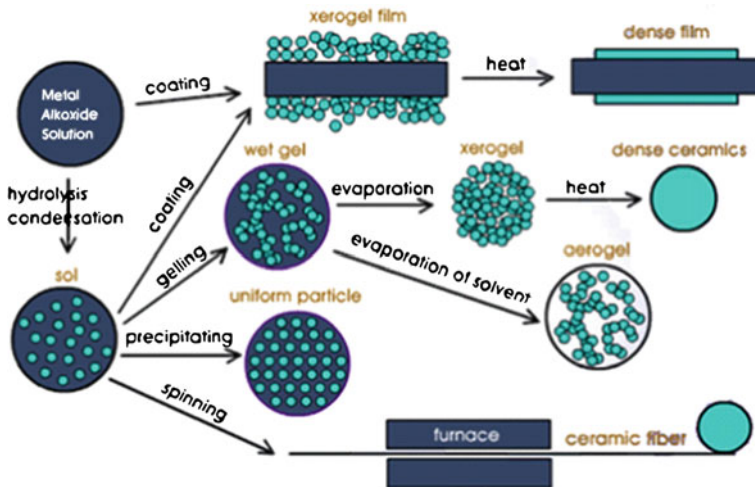


Fig. 2.6 Simplified Chart of sol-gel processes [14]

of microstructure and ease of compositional modification at relatively low temperatures by using simple and inexpensive equipment [15]. Sol-gel techniques have been used not only for powder synthesis or thin-film coating but also for modification of electrode surfaces or electrode/electrolyte interfaces.

## 2.2 SOFC Material Powders Derived from a Sol-Gel Process

The sol-gel method of obtaining ceramic oxide materials has been extensively developed and consists essentially of three steps [15, 16]:

1. Preparation of a starting solution. It involves mixing low viscosity (to ensure homogenization at molecular level) solutions of suitable 'precursors', i.e., metal derivatives; these precursors can in some instances be the 'metal oxide' sols themselves
2. Gelling stage: consists of forming a uniform sol and causing it to gel; this is the key step in the process to endow chemical homogeneity on the ceramic product during desiccation. The transition from the sol to the gel state can be achieved in three different ways:
  - growth of polymeric molecules (which crosslink randomly to a three dimensional network)
  - growth of individual particles (which grow together as they become larger)
  - stabilization of colloids by surface charges (change of the zeta potential and a following interparticle condensation process leads to gelation).

3. Thermal conversion treatment to the final material: shaping during or after gelation into the final form (bulk materials, hollow spheres, fibers, surface coatings, etc.) before firing.

For the preparation of multicomponent ceramic materials, the most commonly employed precursors include metal alkoxides, and other derivatives of metals, such as, metal oxides (sols or solids), nitrates, acetates (carboxylates), and  $\beta$ -diketonates.

Sol-gel techniques have been applied to fabricate SOFC materials with favorable physical and chemical properties that conventional solid state reaction method are unable to provide, which will significantly increase the number of reaction site (TPB) in electrodes or decrease the sintering temperature of the dense electrolyte. More details are described in the following sections.

### 2.2.1 Electrolyte Materials

- Synthesis of YSZ electrolyte powders

The most widely used electrolyte material for SOFCs is yttria-stabilized zirconia (YSZ) with a typical composition of  $(\text{ZrO}_2)_{0.92}(\text{Y}_2\text{O}_3)_{0.08}$  or 8YSZ. The ionic conductivity of YSZ varies with dopant concentration and increases exponentially with temperature [1].

Figure 2.7 illustrates a flow chart for the synthesis of ultrafine YSZ powders through a sol-gel process [17]. The precursors were the zirconium propoxide  $(\text{Zr}(\text{OPr})_4)$  and yttrium nitrate hexahydrate in 1-propanol. After the gelation step at  $50^\circ\text{C}$ , samples were dried at  $80^\circ\text{C}$  for a minimum of 24 h to obtain a xerogel. Then, they were calcined at  $950^\circ\text{C}$  for 2 h. XRD analysis indicates that the obtained powders have a single phase [18]. Figure 2.8 illustrates these nano-structured YSZ powders form an agglomerate with an average primary particle size of 50–100 nm and have nearly spherical morphology. These nano-engineered YSZ particles with controlled morphology and particle size can aid in the packing of particles in the green films and hence enhance sintering kinetics. This, in turn, assists densification of electrolyte films at lower firing temperatures.

- Synthesis of doped ceria electrolyte powders

With high ionic conductivity between 500 and  $700^\circ\text{C}$ , doped cerias have been extensively studied as electrolytes in reduced-temperature SOFCs. Gadolinia-doped ceria (GDC,  $\text{Ce}_{0.9}\text{Gd}_{0.1}\text{O}_{1.95}$ ) is considered to be one of the most promising electrolytes for SOFCs to be operated below  $650^\circ\text{C}$  [19]. Further, doped cerias have also been successfully used as part of anodes for SOFCs, especially those using hydrocarbon fuels [20, 21]. Nano-crystalline GDC powder has been prepared by a sol-gel thermolysis method [20]. After the GDC gel precursors calcined at  $400^\circ\text{C}$ , the powders showed cubic fluorite structure with an average crystallite size



**Fig. 2.7** **a** Procedure of synthesis with AcAc;  
**b** Procedure of synthesis in acid environment [17]

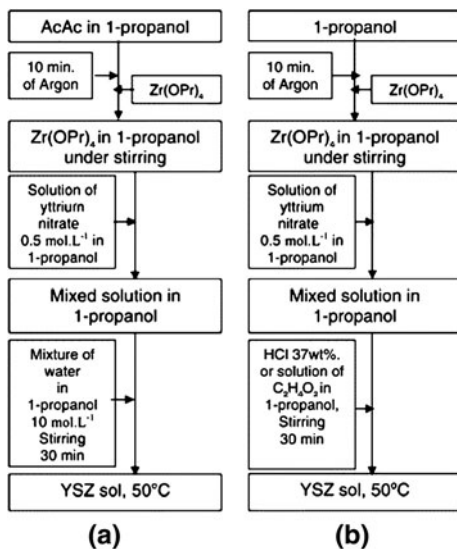
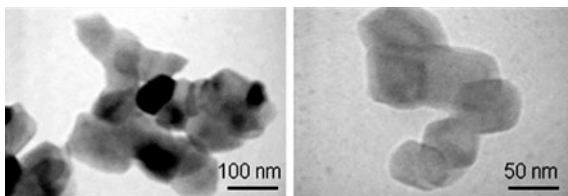


**Fig. 2.8** TEM features of a micrograph of gel calcinated at 400°C with a CA/EG RATIO = 2.4 [18]

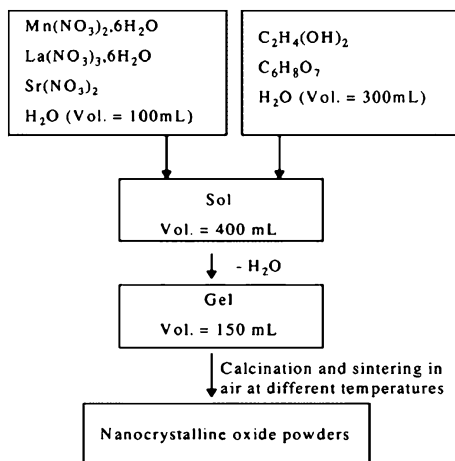


of 10 nm. The powders calcined at lower temperatures showed better sinterability and higher ionic conductivity ( $\sim 2.21 \times 10^{-2} \text{ S cm}^{-1}$  at 700°C in air).

### 2.2.2 Cathode Materials

Sol-gel process has been widely used for synthesis of cathode materials, such as perovskite LSM [22],  $(\text{Pr}_{0.7}\text{Ca}_{0.3})_{0.9}\text{MnO}_{3-\delta}$  [23], Fe-doped LSM [24], LSCF [25, 26],  $\text{Pr}_{1-x}\text{Sr}_x\text{Co}_{0.8}\text{Fe}_{0.2}\text{O}_{3-\delta}$  [27], La, Pr, Sm and/or Ba co-doped  $\text{Ln}_{0.58}\text{Sr}_{0.4}\text{Fe}_{0.8}\text{Co}_{0.2}\text{O}_3$  [28, 29], Sc doped  $\text{SrCoO}_3$  [30], BSCF [31],  $\text{La}_{1-x}\text{Sr}_x\text{CuO}_{3-\delta}$  [32]; layered perovskite oxide of  $\text{PrBaCo}_2\text{O}_{5+\delta}$  [33],  $\text{PrBaCuCoO}_{5+\delta}$  [34],  $\text{GdBaCo}_2\text{O}_{5+\delta}$  [35], and  $\text{K}_2\text{NiF}_4$  type cathode materials  $\text{La}_2\text{Ni}_{1-x}\text{Cu}_x\text{O}_{4+\delta}$  [36],  $\text{La}_{2-x}\text{NiO}_{4+\delta}$  [37] etc. In order to reduce interfacial polarization resistance, an important factor to consider is the grain size of the porous cathode. The TPBs can be increased by decreasing grain size or increasing the surface to volume ratio. Sol-gel process has been studied for the preparation of highly homogeneous and fine cathode powders [38, 39].

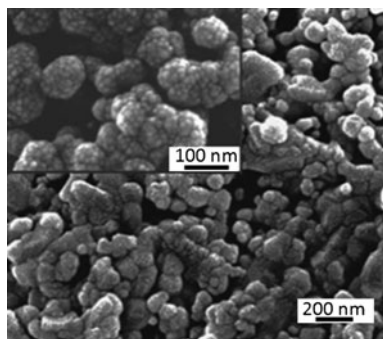
**Fig. 2.9** A flow chart illustrating the processing procedure for LSMx powders preparation [22]



LSM is known to be a classical cathode material for SOFCs based on yttria-stabilized zirconia electrolyte because of its high electrical conductivity, excellent thermal, chemical stability and compatibility with the zirconia-based electrolyte at the working temperatures. Shown in flow chart of Fig. 2.9 is a typical sol-gel process for LSM powders [22]. In this process, the  $\text{La}(\text{NO}_3)_3 \cdot 6\text{H}_2\text{O}$ ,  $\text{Mn}(\text{NO}_3)_2 \cdot 6\text{H}_2\text{O}$  and  $\text{Sr}(\text{NO}_3)_2$  precursors were dissolved into water. Ethylene glycol and citric acid were used as polymerization/complexation agents, respectively. The stable solution was then heated on a thermal plate, where polymerization occurs in the liquid solution and leads to a homogeneous sol. When the sol is further heated to remove the excess solvent, an intermediate resin is formed. Calcination of the resin at  $400^\circ\text{C}$  in air was performed before final sintering at various temperatures ( $600\text{--}1,000^\circ\text{C}$ ). LSM powder has a cubic crystalline structure with particle sizes as small as 40 nm.

Recently, Zhou et al. [40] developed a simple in situ sol-gel derived carbon templating process to synthesize nano-sized  $\text{La}_{0.6}\text{Sr}_{0.4}\text{Co}_{0.2}\text{Fe}_{0.8}\text{O}_{3-\delta}$  (LSCF) and  $\text{La}_{0.8}\text{Sr}_{0.2}\text{MnO}_{3-\delta}$  (LSM). These perovskite oxides were prepared using an EDTA-citrate complexing process to facilitate homogeneous mixing of the metal ions in the molecule level. After calcination of the dried gel under a reducing condition at high temperatures, perovskite oxide and carbon particles were formed simultaneously, producing nano-sized LSCF-carbon and LSM-carbon composites with a grain size of 20–30 nm. Further calcination of the obtained composites in air removes the carbon, resulting in nano-sized LSCF and LSM with a crystalline size of 14 nm, which is smaller than that prepared by the calcination of the solid precursor in air directly (18–22 nm). Such a decrease in crystalline size of perovskite via the indirect calcination process was ascribed to the suppressing effect of carbon in the grain growth of perovskite. Furthermore, when the in situ created carbon was used as a template for pore forming, a highly porous microstructure was obtained. Figure 2.10 shows the typical surface morphology (SEM image) of a sintered pellet [40] with porosity of  $\sim 75\%$ , as determined by the

**Fig. 2.10** Typical surface morphologies of a porous LSCF pellet prepared using the in situ carbon templating process after firing at 1,000°C in air for 5 h [40]



Archimedes method, which is much higher than those obtained from other processes (30–40%). The pores size with irregular pore shape was varied from several  $\mu\text{m}$  to nm while the particle size was in the range of 10–20 nm. The high porosity and high surface area make this in situ carbon templating process very promising for the preparation of porous electrode and catalysts for chemical and energy transformation applications.

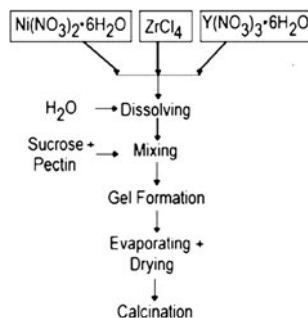
### 2.2.3 Anode and Interconnect Materials

Traditionally anode materials are binary mixtures of nickel (Ni) and yttria-stabilized zirconia (YSZ) particles with a porosity of above  $\sim 30\%$ . Such cermets meet all of the requirements for the anode: the interconnecting Ni network acts as a good catalyst for the electrochemical oxidation of hydrogen and provides an excellent conduction path for electrons released from the electrochemical oxidation of hydrogen; the interconnecting electrolyte material network provides a path for the oxygen ions from the electrolyte and also acts as a constraint for the growth and coalescence of nickel particles so that the fine nickel network could be maintained after long-term operation at elevated temperatures. The performance of the anode, in terms of minimal electrode polarization loss and minimal degradation during operation, depends strongly on its microstructure, and therefore on the precursor powders [41, 42]. It is important that both an ionic conducting network is formed by the YSZ particles and an electronically conducting one is formed by the Ni particles, and that the TPB between the two networks and the gas-phase is long. Furthermore, the relative size of the particles is important, the YSZ particles need to be much smaller than the Ni particles to minimize degradation due to Ni-particle sintering and coarsening during operation [41, 43].

- Synthesis of NiO–YSZ anode powders

The standard way of producing the anode precursor powder mixture is to produce YSZ and NiO particles separately and mix them in a mill [44]. However,

**Fig. 2.11** A flow chart illustrating the preparation of samples [41]



it would be advantageous to produce the powder mixture in one single processing step via a sol-gel process (Fig. 2.11) because the mixing of species occurs on the atomic scale [41], Zirconium tetrachloride ( $\text{ZrCl}_4$ ), yttrium nitrate hexahydrate ( $\text{Y}(\text{NO}_3)_3 \cdot 6\text{H}_2\text{O}$ ), and nickel nitrate hexahydrate ( $\text{Ni}(\text{NO}_3)_2 \cdot 6\text{H}_2\text{O}$ ) were used as precursors. The obtained xerogel is then calcined to obtain NiO/YSZ powder. During calcination this polymeric metal ion complex is decomposed into  $\text{CO}_2$  and  $\text{H}_2\text{O}$ , and their escape from the reaction mixture prevents agglomeration by ensuring that the mixture remains porous. Thus fine particles, which only moderately agglomerated, are formed as the final powder. The Fig. 2.12 illustrated that the agglomerates of NiO/YSZ samples are quite similar in all final powders with different NiO/YSZ ratios. The mean particle sizes of the powders ranging from 28 to 31 nm and a well-crystallized NiO and YSZ powder mixture is formed even for the samples calcined at  $800^\circ\text{C}$ , as indicated by XRD analysis.

- Synthesis of LSCM anode powders

Significant effort has been devoted to the development of anode catalysts for SOFCs run on carbon-containing fuels [45, 46]. For example,  $\text{La}_{0.75}\text{Sr}_{0.25}\text{Cr}_{0.5}\text{Mn}_{0.5}\text{O}_3$  (LSCM) perovskite oxide exhibited excellent redox stability and catalytic activity in both methane and hydrogen SOFCs [47–49]. LSCM powders were prepared using a sol-gel combustion method [50].  $\text{La}(\text{NO}_3)_3$ ,  $\text{Sr}(\text{NO}_3)_2$ ,  $\text{Cr}(\text{NO}_3)_3 \cdot 6\text{H}_2\text{O}$  and  $\text{Mn}(\text{NO}_3)_2 \cdot 6\text{H}_2\text{O}$  salts were first dissolved in deionized water. Then citric acid was added as a chelating agent. After being heated on a hot plate to evaporate water to become dry gel, the resulting powder was calcined at  $1,000^\circ\text{C}$  to prepare LSCM powders. The XRD pattern showed that pure LSCM perovskite oxide was obtained and the TEM image (Fig. 2.13) showed that the average particle size was about 200 nm. Thus, when compared to the powders derived from a solid-state reaction method, the LSCM powders derived from the sol-gel combustion method at a relatively low calcination temperature had uniform morphology [51].

- Synthesis of LMC anode powders

Magnesium doped lanthanum chromate ( $\text{La}_x\text{Mg}_{1-x}\text{CrO}_3$ ) is considered as interconnect material for SOFC applications. The nano powder of this interconnect

**Fig. 2.12** TEM images of the B samples calcined at 800 and 1,000°C [41]

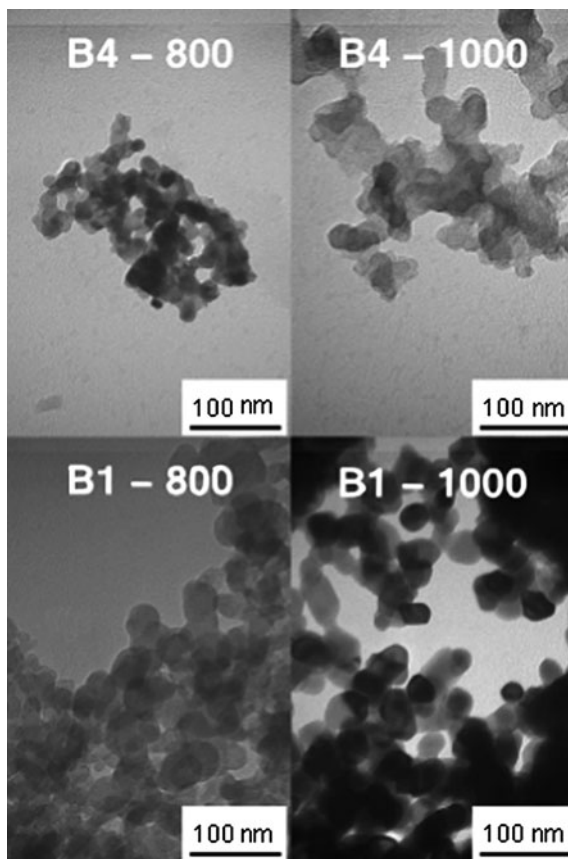
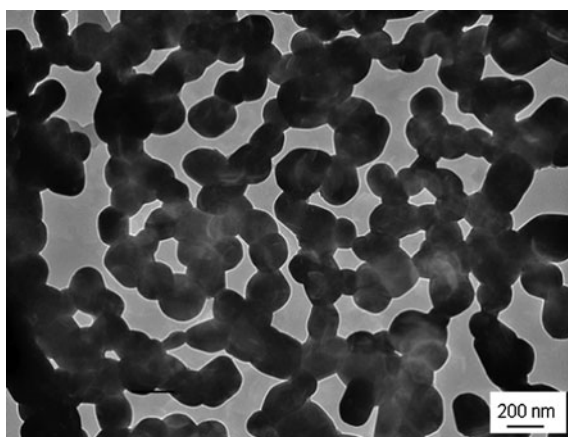


**Fig. 2.13** TEM image of as-prepared LSCM powders [50]



material was prepared using sol-gel process [52]. The precursors were  $\text{La}(\text{NO}_3)_3 \cdot 6\text{H}_2\text{O}$ ,  $4\text{MgCO}_3 \cdot \text{Mg}(\text{OH})_2 \cdot 5\text{H}_2\text{O}$ ,  $(\text{NH}_4)_2\text{Cr}_2\text{O}_7$  and  $\text{Cr}(\text{NO}_3)_3 \cdot 9\text{H}_2\text{O}$  and the chelating agent was citric acid and the dispersant agent was ethylene glycol. The SEM images reveal that the particle size of  $\text{La}_{0.7}\text{Mg}_{0.3}\text{CrO}_3$  powders achieved by sol-gel process is in the range of  $\sim 50\text{--}200$  nm. The powders prepared using  $(\text{NH}_4)_2\text{Cr}_2\text{O}_7$  is more cost-effective than using  $\text{Cr}(\text{NO}_3)_3 \cdot 9\text{H}_2\text{O}$  since it also acts as fuel. The TGA plots depict that there is no further weight loss after reaching 350 and 575°C for the LMC gels prepared using AD and Cr–N, respectively, an indication of complete combustion of the precursors and formation of oxide phases.

## 2.3 Fabrication of SOFC Components Using a Sol-Gel Process

The performance of a SOFC depends strongly on the microstructures of its components. For a single cell, each component should have specific microstructures (in addition to the requirements on intrinsic properties of the materials) in order to achieve high efficiency: a porous, gas-permeable electrode (cathode and anode) with high specific surface area to increase the TPB length and thin, gas-tight electrolyte membrane to reduce the ohmic resistance. Sol-gel process has unique advantages for the fabrication of this kind of ceramic films because it does not require costly equipment, allows a lower processing temperature, and can control microstructure and chemical composition easily. The sol-gel process has been used not only for fabrication of thin electrolyte membranes but also for modification of electrode surfaces and electrode/electrolyte interfaces to improve the microstructure and electrochemical performance of cell components. More details of the sol-gel process for fabrication of cell components are described in the following sections.

### 2.3.1 *Electrolyte*

For efficient operation of a SOFC at low or intermediate temperatures, the electrolyte must be used in a thin-film form to reduce the ohmic losses. Further, the electrolyte membranes must be continuous and crack-free in order to prevent gas leakage, and must rest between two porous electrodes through which gases can pass freely to or away from the active sites for electrochemical reactions near the electrode–electrolyte interface. Thus, the fabrication of defect-free, dense electrolyte films on porous electrodes assumes significant importance.

There are a number of techniques for depositing thin films of ceramics on dense and porous substrates, including chemical vapor deposition, electrochemical vapor deposition, and various sputtering processes using ion beam, magnetron, electron beam, and so forth [53]. The drawbacks of these physical deposition techniques

include difficulties in obtaining good compositional homogeneity [54, 55] and high costs due to the requirements of vacuum conditions [55]. Sol-gel techniques, on the other hand, overcome these problems and offer many additional advantages [56, 57]. Certainly one of the most technologically important aspects of sol-gel process is that, prior to gelation, the fluid sol or solution is ideal for preparing thin films by such common processes as dipping, spinning, or spraying. Both dense and porous structures can be easily tailored through the precursors and there is no limitation on the shape or size of the substrate surface. However, the most important advantage of sol-gel process over conventional coating methods is the ability to control precisely the microstructure (pore volume, pore size, and surface area) and composition (stoichiometry) of the film [58–60]. The disadvantages of sol-gel process include the cost of the raw materials (especially alkoxide precursors), shrinkage that accompanies drying and sintering, and processing times. Thin-film coating is one of the well-known applications of sol-gel process which benefits from most of the advantages of sol-gel process just cited while avoiding these disadvantages [58, 61].

Starting from a molecular precursor, the polymeric sol can be prepared by partial hydrolysis of corresponding metal alkoxide. If the rate of hydrolysis or condensation is very fast, then some kinds of organic acids, beta-dicarbonyls, and alkanolamines have been used as chelating agent in sol-gel processes to control the extent and direction of the hydrolysis-condensation reaction by forming a strong complex with alkoxide. For this reason, extremely thin, dense, and well-defined electrolyte films can be derived from sol-gel coatings on a porous electrode to form an electrode supported SOFC and the thickness can be controlled by the number of applied coatings. Purity and uniformity can also be controlled by the solution chemistry of the sol-gel process.

YSZ films with different thicknesses, such as ultra-thin film (0.1–10  $\mu\text{m}$ ) [53–56] and thick YSZ (8–100  $\mu\text{m}$ ) films [58–60], have been successfully deposited onto dense or porous electrode using a sol-gel process. Since the internal resistance of the cell decreased with decreasing the electrolyte thickness, high performance of 477  $\text{mW}/\text{cm}^2$  at 600°C and 684  $\text{mW}/\text{cm}^2$  at 800°C were achieved in an anode supported SOFC, which consists of a Ni-YSZ anode, a 4YSZ electrolyte (0.5  $\mu\text{m}$ ), and a Pt/Pd cathode Cathode [62]. Other electrolyte materials, such as SDC [61], BCG [63], zirconia films doped with  $\text{Sc}_2\text{O}_3$  and  $\text{Al}_2\text{O}_3$  (85 mol.%  $\text{ZrO}_2$ -11 mol.%  $\text{Sc}_2\text{O}_3$ -4 mol.%  $\text{Al}_2\text{O}_3$ ) [64], have also been successfully fabricated via a sol-gel process.

Sol-gel process was also used for preparing an electronic blocking layer, such as thin YSZ layer, on doped ceria electrolyte to enhance the OCV [65–67]. Kim et al. [67] successfully fabricated 2  $\mu\text{m}$  thick YSZ layer on YDC electrolyte surface using a sol-gel spin coating method. The open circuit voltage (OCV) of a single cell based on this composite electrolyte was  $\sim 0.5$  V higher than that for an uncoated YDC electrolyte at temperatures from 700 to 1,050°C. The maximum power density of the single cell with the bi-layer electrolyte was 122  $\text{mW}/\text{cm}^2$  at 800°C, comparable to that of an YSZ single cell with the same electrolyte thickness at 1,000°C ( $\sim 144$   $\text{mW}/\text{cm}^2$ ).

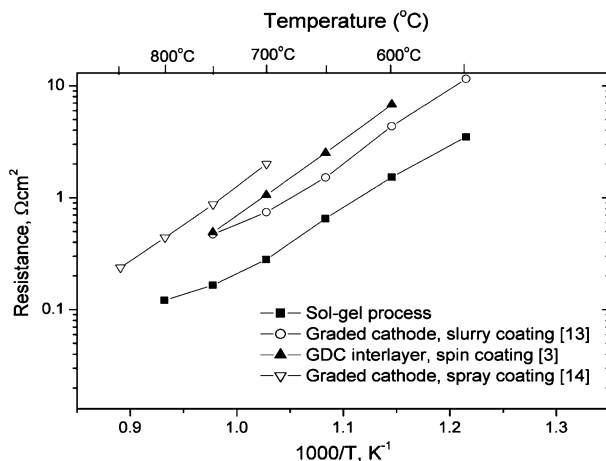


**Fig. 2.14** Interfacial polarization resistances of LSM-GDC electrodes on a YSZ electrolyte prepared by different processes [71]

Another application of sol-gel process is to enhance the density of the YSZ layer through sol-gel coating on the prepared YSZ layer [68, 69] using other ceramic process. Burgess et al. [68] found that the sol-gel coated YSZ layer reduced the gas permeation through the electrolyte layers by up to 37% after firing to 500 or 650°C compared to that of YSZ layer (prepared by plasma spray YSZ coating). The sol-gel coatings led to a substantial increase in OCV and a small decrease in series resistance due to the decreased porosity of the electrolytes and a large decrease in polarization resistance due to increased interfacial surface area. Sol-gel coating has been also tried to remove defects produced after the slurry coating of YSZ on a porous anode [69].

### 2.3.2 Cathode

One of the most important goals in SOFC research is the reduction of the working temperature from high temperature (such as 900–1,000°C) to intermediate temperature (500–800°C) for future applications. However, at intermediate temperature, one of the main limiting factors is the high polarization resistance of the cathode, which limits SOFC power densities. In order to improve the cathode performance, the cathode has to be porous and have a small grain size to optimize the active surface area and the TPB length [70]. Sol-gel process is ideally suited for assembling such microstructures. The advantages of a sol-gel process over other technologies include: (i) the microstructure and composition of electrode materials can be controlled with relative ease, (ii) the electrode and electrolyte adherence is strong, and (iii) low-temperature processing is possible.



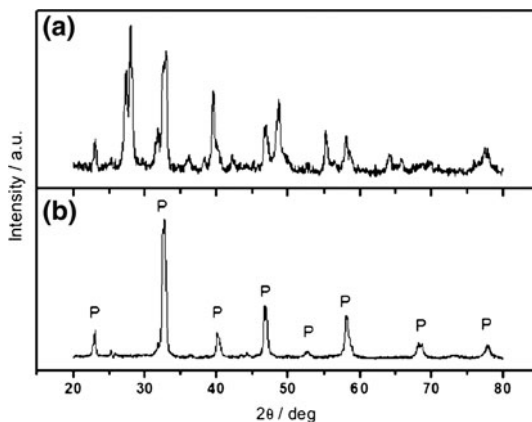
Xia et al. [71] developed a modified sol-gel process to fabricate LSM/GDC composite cathode for honeycomb SOFCs based on stabilized zirconia electrolytes. The sol-gel process derived cathodes show much lower interfacial polarization resistances than those prepared by slurry coating or spray deposition (shown in Fig. 2.14). The interfacial polarization resistances were 0.65 and 0.16  $\Omega \text{ cm}^2$  at 650 and 750°C, respectively, as determined using impedance spectroscopy. The high performance suggested that the sol-gel process has the advantage of developing strong bonding between the electrode and electrolyte at low temperatures and achieving desirable microstructures for fuel cell electrodes: small grains, high porosity, large surface area, and long TPB.

It is believed that cathode performance can be improved by using a thin layer with flat surface and small grains diameter at the cathode/electrolyte interface, covered by a thicker and porous layer with larger grains. This duplex microstructure design will increase the reaction zone and ensures the current collection by the additional porous layer [37]. Under this guidance, Fontaine et al. [37] developed thin graded porosity and composition of  $\text{La}_{2-x}\text{NiO}_4$  ( $x \geq 0$ ) cathode interlayer onto YSZ substrates using a sol-gel process. Through careful control of organic concentration, the ratio of transition metals, the number of coats, and the withdrawal speed, homogeneous, crack-free, and porous  $\text{La}_{2-x}\text{NiO}_4$  ( $x \geq 0$ ) films were successfully fabricated by dip-coating the sol onto YSZ substrates. The results indicated that low organic concentration allows the synthesis of cathode interlayer with fine microstructure and spherical grain of about 50 nm, while coarse microstructure with platelets is obtained for higher concentration. The film thickness was influenced by the number of coatings and the withdrawal speed. Controlled both film microstructure and composition can be easily achieved by changing processing parameters. Unfortunately, the authors did not report the electrochemical properties of the interlayer derived from the sol-gel process.

Sol-gel process is an ideal tool for functionally graded multilayer structure formation. Functionally graded 4-layer cathode was prepared by sol-gel/slurry coating [72]. The interlayer in contact with the electrolyte consisted of 50% LSM and 50% GDC and the composition was changed from a catalytically active layer to a current collection layer. The particulate sol of GDC was prepared and then the sol was mixed with LSM or other current collecting materials to produce the slurry for multilayer coating. The cathode interfacial polarization resistances for this graded cathode fired at 900°C are 0.21 and 0.10  $\Omega \text{ cm}^2$  at 700 and 800°C, respectively.

Another advantage of the sol-gel process is lower processing temperature, avoiding undesirable reaction between electrolyte and cathode materials. The cathode materials, such as lanthanum strontium cobalt ferrite (LSCF), strontium-doped samarium cobaltite (SSC), have attracted increasing attention for intermediate temperature SOFC due to their mixed-conduction characteristics and relatively high ionic conductivity. However, those materials have a strong tendency to react with YSZ to form insulating phases, like  $\text{La}_2\text{Zr}_2\text{O}_7$  or  $\text{SrZrO}_3$ , at the cathode-electrolyte interface at high temperatures. Sol-gel can significantly reduce the sintering temperature of the cathode. Tang et al. [73] successfully prepared

**Fig. 2.15** XRD patterns of the decomposition products from LSM precursors (a) without and (b) with Triton X-100, sintered at 800°C for 1 h. [75]



200 nm thick SSC film on YSZ using dip-coating from the alkoxide precursor solution modified with an organic polymer (polyethylene glycol (PEG)). They found single-perovskite phase SSC films were formed when the films were heated at 700°C, and the crystalline size of the SSC film was around 50–100 nm when PEG was added. Other materials, like strontium-substituted lanthanum ferromanganites,  $\text{La}_{0.8}\text{Sr}_{0.2}\text{Mn}_{1-y}\text{Fe}_y\text{O}_z$  ( $y = 0, 0.2, 0.5, 0.8, 1$ ), LSMF2Y ( $Y = 10y$ ) films have been synthesized by a polymeric sol-gel route and deposited on YSZ substrates by a dip-coating process [24].

Sol-gel process has also been widely used for cathode infiltration, such as YSZ or SDC infiltrated LSM [74], LSM infiltrated YSZ [75], copper manganese spinel infiltrated YSZ [76]. Sholklafter et al. [75] carefully studied the phase formation for the LSM infiltrated YSZ. They found that the addition of the commercial polymeric dispersant to the nitrate precursors facilitated the formation of perovskite LSM particles at low temperatures. Figure 2.15 displays XRD patterns for the nanoscale synthesis of  $\text{La}_{0.85}\text{Sr}_{0.15}\text{MnO}_3$ , with and without the surfactant Triton X-100. As indicated in Fig. 2.15a, directly decomposing the nitrate precursors at 800°C did not yield a phase-pure LSM perovskite. In contrast, in the presence of the surfactant, the majority of characteristic peaks in Fig. 2.15b correspond to the LSM perovskite phase. Presumably, the surfactant has the effect of complexing the metal ions, so that the individual oxides do not form prematurely. Such complexing effects are well known in a sol-gel process.

### 2.3.3 Anodes

More recently, metal supported cells, which uses metal mechanical support deposited with ceramic active materials (anode, electrolyte and cathode), have been developed for a new generation of fuel cells [77, 78]. However, the use of metallic material as cell support induces thermal limitations such as the decrease in

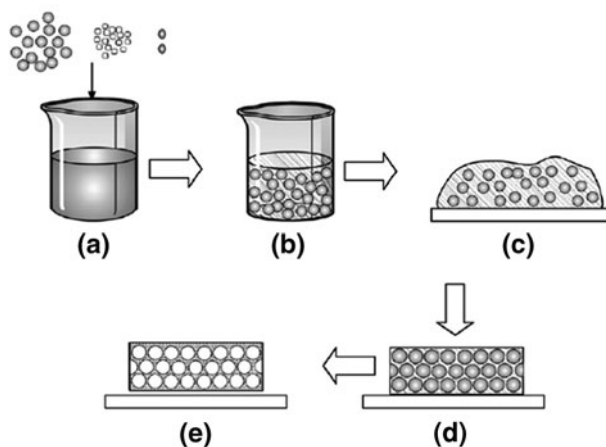


**Fig. 2.16** Schematic diagram of the preparation of thin layer materials with macroporous microstructure. Starting metal salts are dissolved in distilled water, citric acid was used as complexing agent and PMMA microspheres as pore former (a). The homogeneous suspension (b) is deposited on a substrate (c) rendering an ordered template of PMMA microspheres with an infiltrated citrate gel of stoichiometric cations (d). An inorganic porous microstructure is obtained after calcination (e) [81]

anodic material sintering temperature. Indeed, a heat thermal treatment above 800°C would damage metal support, either mechanically or by corrosion. Rieu et al. [79, 80] successfully prepared both thin (around 100 nm) and thick (10–20  $\mu\text{m}$ ) NiO–YSZ anodic film on dense and porous metallic supports. A low thermal treatment at only 800°C leads to a coherent anodic duplex stacking which is continuous, homogeneous and adherent.

### 2.3.4 Other Components Derived from a Sol-gel Process

Sol-gel process is also employed to prepare thin layer oxides with controlled macroporous microstructure for SOFC applications [81]. Shown in Fig. 2.16 is the schematic diagram of the preparation of the thin layer materials. The method uses aqueous stoichiometric cation solutions of metal nitrates, citric acid as complexing agent and polymethyl methacrylate (PMMA) microspheres as pore former. They have successfully prepared several mixed oxides with fluorite and perovskite-type structures, i.e. doped zirconia, ceria, ferrites, manganites, and NiO–YSZ composites. The synthesized materials are nanocrystalline and have a homogeneous pore distribution and relatively high specific surface area. Some of the microstructures are presented in Figs. 2.17 and 2.18. Homogeneous and ordered pore arrangement with uniform wall thickness were achieved for all of the samples. The specific structure of the macroporous microstructure makes them interesting for SOFC and catalysis applications in the intermediate temperature range.

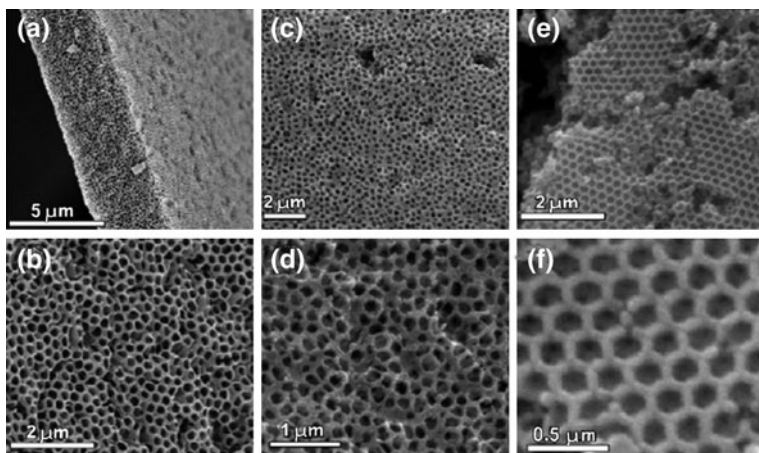


**Fig. 2.17** SEM images of the different electrolytes: **a** and **b** cross-section and surface view, respectively of the YSZ layers; **c** and **d** surface of LMO at different magnifications; **e** and **f** surface of CGO at different magnifications [81]

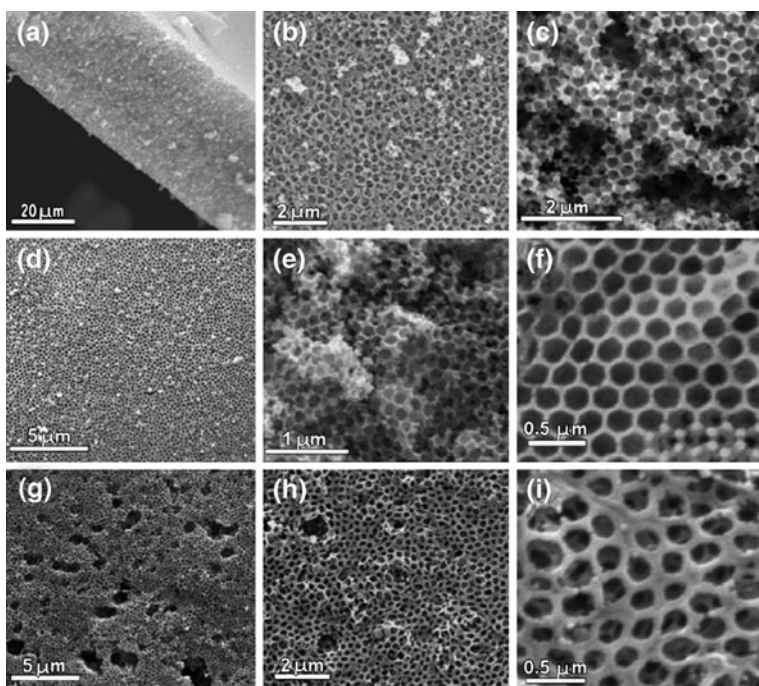


**Fig. 2.18** SEM images revealing the microstructural details of the surface and cross-section view of different electrodes: **a–c** LSM, **d–f** LSF and **g–i** LSTMG [81]

In summary, the sol-gel technique has been widely used in recent years to form fuel cell components with enhanced microstructures for SOFCs. Both dense and porous structure can be easily tailored through the precursors and there is no limitation in the shape or size of the substrate surface. However, the sol-gel method also has some disadvantages such as a complex synthesis route; the quality of the coating was influenced much by many process parameters. And the typical gels show inherently large shrinkage, usually 20–25 vol%, which will introduce huge shrinkage stresses during drying/heating process. For a thick film application, in order to avoid crack formation, coating and drying/heating processes have to be repeated several times to get the designed thickness, which is time-, labor- and energy-intensive process. The sol-gel process also needs further development to deposit micro-structured materials in a selective area such as the triple-phase boundary of a fuel cell.

## 2.4 Surface Modification by a Sol-Gel Process

As mentioned in Sect. 2.3, ultra-thin coating can be easily achieved using a sol-gel process and the coating process is not limited by the shape and size of the substrates. Up to now, sol-gel processes have been successfully employed in SOFCs to enhance the performance and stability of the components.

### 2.4.1 Enhance Cathode Performance and Stability Through Surface Medication

In recent years,  $\text{La}_x\text{Sr}_{1-x}\text{Co}_y\text{Fe}_{1-y}\text{O}_{3-\delta}$  (LSCF)-based cathodes have attracted much attention due to its much higher ionic and electronic conductivity than the conventional LSM cathode [82–84] and higher performance have been achieved in the temperature range of 600–800°C. However, the electrochemical activity of the stand-alone LSCF cathode is likely to be limited by the surface catalytic properties [85, 86]. The dominant oxygen reduction reaction is associated with the surface exchange process [87]. Inadequate long-term stability of LSCF is also a primary factor impeding the widely practical commercial application [88–90]. In order to enhance the performance and/or stability of LSCF cathode, Liu et al. proposed to improve the performance and stability of a porous LSCF cathode by the application of a thin, catalytically active coating through infiltration [91], as schematically shown in Fig. 2.19. The new electrode structure can make effective use of desirable properties of two different materials: fast ionic and electronic transport in the backbone of LSCF cathode and facile surface kinetics on the thin surface coating. The coating could be a discontinuous porous layer or a continuous dense film.

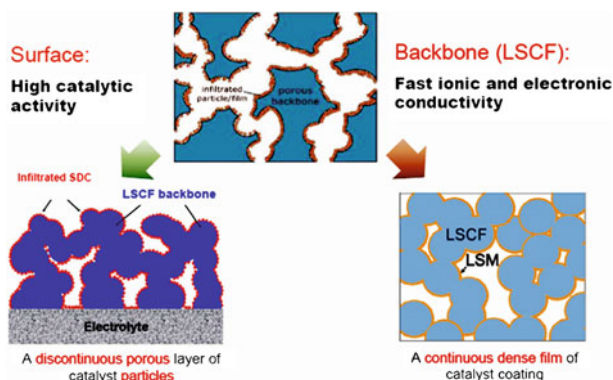


Fig. 2.19 Schematics of catalyst-infiltrated LSCF cathodes

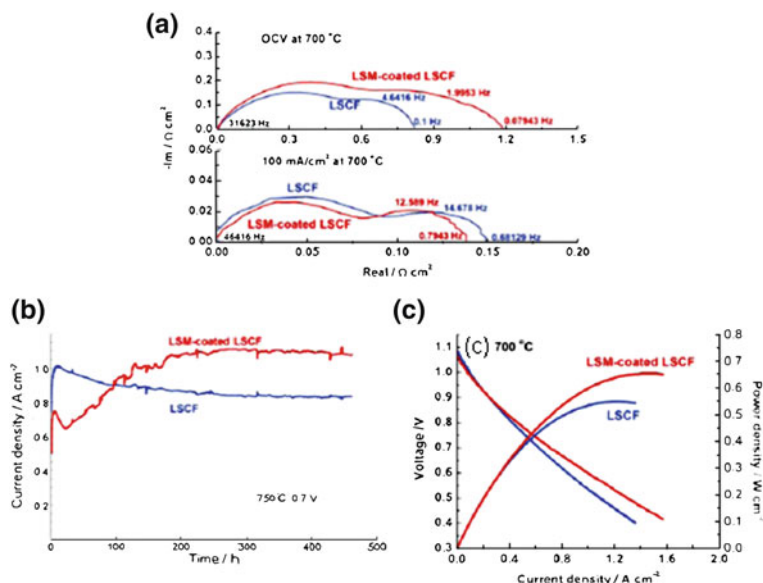


Fig. 2.20 **a** Interfacial impedance  $\{Z_{\text{cell}} - Z_b\}$  of fuel cells with and without infiltration of LSM measured at OCV and at 100 mA cm<sup>-2</sup>. **b** Current density of two test cells with and without infiltration as a function of time at a constant voltage of 0.7 V and approximate cathodic overpotential of -0.12 V. **c** Cell voltages and power densities as a function of current density for full cells with and without infiltration of LSM after long-term testing [92]

Improved performance and stability has been reported by using thin catalytic coating of LSM [92], SSC [93] and SDC [94] on LSCF surface. For example, Matt et al. [92] systematically studied the electrochemical behavior of LSM infiltrated LSCF cathode. The thin coating of LSM on the LSCF surface significantly enhanced the long-term stability and performance, as shown in Fig. 2.20. The thin



LSM film formation on LSCF surface and stability of LSM/LSCF were carefully discussed by Choi et al. [95]. In the SDC infiltrated LSCF cathode, Nie et al. [94] found that the microstructures and performances of SDC infiltrated LSCF cathodes depend sensitively on the amount of SDC introduced and the microstructure of the SDC coatings. With 10  $\mu\text{L}$  of 0.25 mol/L SDC infiltrated into LSCF cathode, the interfacial resistance reduced to about half of those for the blank cathode, implying 50% improvement of the electrochemical performance. Short term stability (about 100 h tests) in the anode supported cell indicated that the SDC infiltrated LSCF can significantly improve the performance and stability; however, the detailed mechanism is yet to be determined. Yoon et al. [74] deposited a YSZ or samaria-doped ceria ( $\text{Sm}_{0.2}\text{Ce}_{0.8}\text{O}_2$ , SDC) film at the triple-phase boundary (TPB) of LSM/YSZ/gas to increase the number of electrochemical reaction sites, which resulted in a decrease of cathode polarization and increase of cell performance. A maximum power densities of the cell modified by the SDC sol-gel coating were about  $0.53 \text{ W/cm}^2$  at  $750^\circ\text{C}$  and about  $0.19 \text{ W/cm}^2$  at  $650^\circ\text{C}$  [74].

#### ***2.4.2 Modification of Porous Anodes for Sulfur and Carbon Tolerance***

One of the major advantages of SOFCs is the fuel flexibility. A wide variety of practical hydrocarbons such as methane, propane, gasoline, diesel and kerosene can be direct utilized as the fuels in SOFCs [2, 3, 96–98]. The direct utilization of hydrocarbon fuels will increase the operating efficiency and reduce system costs, which will accelerate substantially the use of SOFCs in transportation, residential, and distributed-power applications. The conventional anode for a SOFC, a composite consisting of nickel and yttria-stabilized zirconia, has excellent catalytic activity for fuel oxidation, good conductivity for current collection, and matched compatibility with YSZ electrolyte for easy cell fabrication, but it is highly susceptible to carbon buildup (coking) and deactivation (sulfur poisoning) by contaminants commonly encountered in readily available fuels [2].

To overcome these problems, substantial effort has been devoted to the development of new anode materials and novel electrode structures. Though some new anode materials have been developed with improved tolerance, such as Cu-based cermet [99–101],  $\text{La}_{0.75}\text{Sr}_{0.25}\text{Cr}_{0.5}\text{Mn}_{0.5}\text{O}_3$  [47],  $\text{Sr}_2\text{Mg}_{1-x}\text{Mn}_x\text{MoO}_6$  ( $0 \leq x \leq 1$ ) [102], doped  $(\text{La},\text{Sr})(\text{Ti})\text{O}_3$  [103, 104], and  $\text{La}_{0.4}\text{Sr}_{0.6}\text{Ti}_{1-x}\text{Mn}_x\text{O}_3$  [105], their practical application is stalled by other problems such as low electronic conductivity, poor electrochemical activity, and limited physical, chemical, and thermal compatibility with YSZ electrolyte. An effective approach is using a catalytic coating to modify the Ni–YSZ surface to enhance the coking and sulfur tolerance. Yoon et al. [106] used a coating of SDC sol to modify the Ni–YSZ anode for hydrocarbon fuel. The surface modification of Ni/YSZ anode resulted in an increase of structural stability and enlargement of the TPB, which served as a catalytic reaction site for oxidation of carbon or carbon monoxide. Maximum power density of  $0.3 \text{ W/cm}^2$  was

achieved at 700°C using the mixture of methane (25%) and air (75%) as the fuel and air as the oxidant and the cell was operated for 500 h without significant degradation of cell performance [106]. Yang et al. [2] developed a catalyst material of BZCYYb, which shows high water adsorption capability at high temperatures. With BZCYYb infiltrated into NiO–YSZ anode, the cell showed a stable power output for 1,000 h in wet hydrogen contaminated with 10 ppm H<sub>2</sub>S, implying that BZCYYb exhibits considerable stability for long-term sulfur tolerance, and the sulfur poisoning can be fully suppressed in the presence of a small amount of steam.

### ***2.4.3 Protective Coatings for Metallic Interconnect***

Metallic interconnects are preferred over the conventional ceramic interconnects, for planar-type SOFC, due to their superior electronic and heat conductivity and low-cost. Among these alloys, Cr<sub>2</sub>O<sub>3</sub>-forming ferritic stainless steel were one of the most promising candidates due to close match of their coefficients of thermal expansion (CTE) to those of the cell components. However, the long-term stability of the metallic interconnects and the compatibility issues are still a concern. For example, over long-term exposure during SOFC operation, Cr<sub>2</sub>O<sub>3</sub> oxide will thermally grow on the surface and increase the electrical resistance. Additionally, the volatile Cr species, primarily in the form of CrO<sub>3</sub> or CrO<sub>2</sub>(OH)<sub>2</sub>, generated from Cr<sub>2</sub>O<sub>3</sub> tends to deposit on the surface of cathode and/or the interface between cathode and electrolyte, forming a double-layer oxide scale structure of (Mn, Cr)<sub>3</sub>O<sub>4</sub> spinel on top of Cr<sub>2</sub>O<sub>3</sub>, which leads to a significant decrease in cathode activity and subsequent the stack performance [107, 108]. To solve these potential problems, using surface modification via application of a protective coating of conductive oxides is an effective approach to enhance oxidation resistance, surface stability, scale adhesion and conductivity as well as alleviate Cr vaporization [107–109]. Zhu et al. [107] successfully applied a LaCrO<sub>3</sub> thin film on a ferritic stainless steel substrate via sol-gel coating process. The LaCrO<sub>3</sub> coating provided effective protection for the interconnect steel during oxidation of twelve 100 h cycles at 800°C in air, whereas significant spallation and weight loss were observed for the uncoated steel. Pu et al. [108] investigated the oxidation behavior and the microstructure of the SUS 430 ferritic stainless steel in air at 800°C for 200 h. They found that a NiCo<sub>2</sub>O<sub>4</sub> protective coating prepared by sol-gel process can significantly increase the oxidation resistance of the SUS 430 alloy by limiting the access of O<sub>2</sub> in air to the outwardly diffused cations, while the electrical conductivity is considerably improved due to inhibited growth of resistive Cr<sub>2</sub>O<sub>3</sub> and the formation of conductive spinel phases in the oxide scale. The parabolic rate constant of the oxidation kinetics is  $8.1 \times 10^{-15} \text{ g}^2 \text{ cm}^{-4} \text{ s}^{-1}$  for the coated specimen, in comparison with  $8.3 \times 10^{-14} \text{ g}^2 \text{ cm}^{-4} \text{ s}^{-1}$  of the uncoated. Hua et al. [110] successfully prepared a MnCo<sub>2</sub>O<sub>4</sub> protective coating on SUS 430 alloy by a sol-gel process. They found that the best technique for forming the MnCo<sub>2</sub>O<sub>4</sub> protective coating was calcined in reducing atmosphere followed by



pre-oxidation in the air, which enhances the oxidation resistance, and improves the electrical conductivity and adherence of coated SUS 430 alloy significantly. As a result, the  $\text{MnCo}_2\text{O}_4$  spinel is the most potential candidate for SOFC metallic interconnect protective coating application [109].

## 2.5 Summary

SOFCs have attracted worldwide attention because of their high energy efficiency and excellent fuel flexibility. The performance of SOFCs depends sensitively on the microstructures of cell components. For example, the electrodes (both cathode and anode) must be porous and gas-permeable to minimize resistance to gas transport and have high specific surface area to increase the number of active sites (such as TPBs) for electrochemical reactions. In contrast, the electrolyte membrane must be thin to reduce the ohmic loss and gas-tight (or dense) to prevent gas leakage. A sol-gel process has unique advantages for the fabrication of SOFC materials and components with desired microstructures. Further, it is cost-effective because it does not require costly equipment, allows lower processing temperature, and can easily control the chemical composition. Both dense and porous structures can be easily tailored and there is no limitation on the shape or size of the substrate surface. Sol-gel processes have also been successfully applied to preparation of highly homogeneous and fine powders and to modification of electrode surface or electrode/electrolyte interfaces.

However, sol-gel techniques also have some disadvantages: some synthesis routes may be complex, some processes can be time-consuming, precursors are often expensive and sensitive to moisture; and the quality of the coating may be influenced sensitively by many processing parameters. Sol-gel processes also need further development for deposition of nanostructured materials in a selective area such as the triple-phase boundary of a fuel cell. Finally, the problems of dimensional change on densification, and of shrinkage and stress cracking on drying, although not insurmountable, do require careful attention. These significant limitations underline the need for sol-gel process optimization to exploit their advantages to the maximum in applications where they can provide properties not attainable by other methods, including fabrication of thin-film electrolyte membranes and functionally graded multilayer electrode structures, infiltration of catalyst/electrode coatings onto scaffolds, and surface modification of electrodes for enhanced performance and stability.

## References

1. Minh NQ, Takahashi T (1995) Science and technology of ceramic fuel cells. Elsevier, Amsterdam
2. Yang L, Wang SZ, Blinn K, Liu MF, Liu Z, Cheng Z, Liu ML (2009) Enhanced sulfur and coking tolerance of a mixed ion conductor for SOFCs:  $\text{BaZr}_{0.1}\text{Ce}_{0.7}\text{Y}_{0.2-x}\text{Yb}_x\text{O}_{3-\delta}$ . Science 326(5949):126–129

3. Yang L, Choi Y, Qin W, Chen H, Blinn K, Liu M, Liu P, Bai J, Tyson TA, Liu M (2011) Promotion of water-mediated carbon removal by nanostructured barium oxide/nickel interfaces in solid oxide fuel cells. *Nat Commun* 2:357
4. Zhe C, Wang JH, Choi YM, Yang L, Lin MC, Liu M (2011) From Ni-YSZ to sulfur-tolerant anodes: electrochemical behavior, modeling, in situ characterization, and perspectives. *Energy Environ Sci Perspect Rev* 4:4380–4409
5. Singhal SC (2000) Science and technology of solid-oxide fuel cells. *MRS Bull* 25(3):16–21
6. Liu M, Lynch ME, Blinn K, Alamgir F, Choi Y (2011) Rational SOFC material design: new advances and tools. *Mat Today Invited Rev* 14:534–546
7. [http://science.nasa.gov/headlines/y2003/18mar\\_fuelcell.htm](http://science.nasa.gov/headlines/y2003/18mar_fuelcell.htm)
8. [http://www.doitpoms.ac.uk/tlplib/fuel-cells/high\\_temp\\_sofc.php](http://www.doitpoms.ac.uk/tlplib/fuel-cells/high_temp_sofc.php)
9. <http://www.aki.che.tohoku.ac.jp/~koyama/html/research/SOFC.html>
10. Ormerod RM (2003) Solid oxide fuel cells. *Chem Soc Rev* 32(1):17–28
11. Xia CR, Liu ML (2002) Novel cathodes for low-temperature solid oxide fuel cells. *Adv Mat* 14(7):521
12. (2005) 2004 fuel cell handbook: advanced technology for generating electricity series on renewable energy, biofuels, bioenergy, and biobased products, US Department of Energy, 7th edn. Progressive Management
13. [http://www.doitpoms.ac.uk/tlplib/fuel-cells/sofc\\_electrode\\_materials.php](http://www.doitpoms.ac.uk/tlplib/fuel-cells/sofc_electrode_materials.php)
14. Pierre AC (1998) Introduction to sol-gel processing. Springer, London
15. Brinker CJ, Scherer GW (1990) Sol-gel science: the physics and chemistry of sol-gel processing, 1st edn. Academic Press
16. Mehrotra RC (1989) In: Aegerter MA, Souza Jr., DF, Zanotto ED (eds) Sol-gel science and technology. World Scientific Publishing Company, Singapore
17. Viazzi C, Deboni A, Ferreira JZ, Bonino JP, Ansart F (2006) Synthesis of Yttria Stabilized Zirconia by sol-gel route: Influence of experimental parameters and large scale production. *Solid State Sci* 8(9):1023–1028
18. Laberty-Robert C, Ansart F, Deloget C, Gaudon M, Rousset A (2001) Powder synthesis of nanocrystalline  $\text{ZrO}_2\text{--}8\%\text{Y}_2\text{O}_3$  via a polymerization route. *Mat Res Bull* 36(12):2083–2101
19. Steele BCH (2000) Appraisal of  $\text{Ce}_{1-x}\text{Gd}_x\text{O}_{2-y/2}$  electrolytes for IT-SOFC operation at 500 degrees C. *Solid State Ion* 129(1–4):95–110
20. Prasad DH, Son JW, Kim BK, Lee HW, Lee JH (2008) Synthesis of nano-crystalline  $\text{Ce}_{0.9}\text{Gd}_{0.1}\text{O}_{1.95}$  electrolyte by novel sol-gel thermolysis process for IT-SOFCs. *J Eur Ceram Soc* 28(16):3107–3112
21. Mogensen M, Sammes NM, Tompsett GA (2000) Physical chemical and electrochemical properties of pure and doped ceria. *Solid State Ion* 129(1–4):63–94
22. Gaudon M, Laberty-Robert C, Ansart F, Stevens P, Rousset A (2002) Preparation and characterization of  $\text{La}_{1-x}\text{Sr}_x\text{MnO}_{3+\delta}$  ( $0 \leq x \leq 0.6$ ) powder by sol-gel processing. *Solid State Sci* 4(1):125–133
23. Xiong L, Wang SR, Wang YS, Wen TL (2008)  $(\text{Pr}_{0.7}\text{Ca}_{0.3})_{(0.9)}\text{MnO}_{3-\delta}$ -SDC cathode for IT-SOFC. *J Alloy Compd* 453(1–2):356–360
24. Lenormand P, Castillo S, Gonzalez JR, Laberty-Robert C, Ansart F (2005) Lanthanum ferromanganites thin films by sol-gel process. Influence of the organic/inorganic R ratio on the microstructural properties. *Solid State Sci* 7(2):159–163
25. Ghouse M, Al-Yousef Y, Al-Musa A, Al-Otaibi MF (2010) Preparation of  $\text{La}_{0.6}\text{Sr}_{0.4}\text{Co}_{0.2}\text{Fe}_{0.8}\text{O}_3$  nanoceramic cathode powders for solid oxide fuel cell (SOFC) application. *Int J Hydrogen Energy* 35(17):9411–9419
26. Ding C, Lin H, Sato K, Hashida T (2008) Synthesis and characterization of  $\text{La}_{0.8}\text{Sr}_{0.2}\text{Co}_{0.8}\text{Fe}_{0.2}\text{O}_3$  nanoparticles for intermediate-low temperature solid oxide fuel cell cathodes. *Water Dyn* 987:35–38
27. Meng XW, Lu SQ, Ji Y, Wei T, Zhang YL (2008) Characterization of  $\text{Pr}_{1-x}\text{Sr}_x\text{Co}_{0.8}\text{Fe}_{0.2}\text{O}_{3-\delta}$  ( $0.2 \leq x \leq 0.6$ ) cathode materials for intermediate-temperature solid oxide fuel cells. *J Power Sources* 183(2):581–585

28. Vert VB, Serra JM (2009) Influence of Barium incorporation on the electrochemical performance of  $\text{Ln}_{0.58}\text{Sr}_{0.4}\text{Fe}_{0.8}\text{Co}_{0.2}\text{O}_{3-\delta}$  ( $\text{Ln} = \text{La}, \text{Pr}, \text{Sm}$ ) Perovskites for oxygen activation at intermediate temperatures. *Fuel Cells* 9(5):663–678
29. Vert VB, Serra JM (2010) Improvement of the Electrochemical Performance of  $\text{Ln}_{0.58}\text{Sr}_{0.4}\text{Fe}_{0.8}\text{Co}_{0.2}\text{O}_{3-\delta}$  IT-SOFC Cathodes by Ternary Lanthanide Combinations (La-Pr-Sm). *Fuel Cells* 10(4):693–702
30. Zeng PY, Ran R, Zhihao CAH, Zhou W, Gu HX, Shao ZP, Liu SM (2008) Efficient stabilization of cubic perovskite  $\text{SrCoO}_{3-\delta}$  by B-site low concentration scandium doping combined with sol-gel synthesis. *J Alloy Compd* 455(1–2):465–470
31. Shao ZP, Haile SM (2004) A high-performance cathode for the next generation of solid-oxide fuel cells. *Nature* 431(7005):170–173
32. Zheng MZ, Liu XM, Su WH (2005) Preparation and performance of  $\text{La}_{1-x}\text{Sr}_x\text{CuO}_{3-\delta}$  as cathode material in IT-SOFCs. *J Alloy Compd* 395(1–2):300–303
33. Zhao L, He BB, Lin B, Ding HP, Wang SL, Ling YH, Peng RR, Meng GY, Liu XQ (2009) High performance of proton-conducting solid oxide fuel cell with a layered  $\text{PrBaCo}_2\text{O}_{5+\delta}$  cathode. *J Power Sources* 194(2):835–837
34. Zhao L, Nian Q, He BB, Lin B, Ding HP, Wang SL, Peng RR, Meng GY, Liu XQ (2010) Novel layered perovskite oxide  $\text{PrBaCuCoO}_{5+\delta}$  as a potential cathode for intermediate-temperature solid oxide fuel cells. *J Power Sources* 195(2):453–456
35. Pena-Martinez J, Tarancon A, Marrero-Lopez D, Ruiz-Morales JC, Nunez P (2008) Evaluation of  $\text{GdBaCo}_2\text{O}_{5+\delta}$  as Cathode Material for Doped Lanthanum Gallate Electrolyte IT-SOFCs. *Fuel Cells* 8(5):351–359
36. Ferkhi M, Khelili S, Zerroual L, Ringuede A, Cassir M (2009) Synthesis, structural analysis and electrochemical performance of low-copper content  $\text{La}_2\text{Ni}_{1-x}\text{Cu}_x\text{O}_{4+\delta}$  delta materials as new cathodes for solid oxide fuel cells. *Electrochim Acta* 54(26):6341–6346
37. Fontaine ML, Laberty-Robert C, Ansart F, Tailhades P (2006) Composition and porosity graded  $\text{La}_{2-x}\text{NiO}_{4+\delta}$  ( $x \geq 0$ ) interlayers for SOFC: Control of the microstructure via a sol-gel process. *J Power Sources* 156(1):33–38
38. Livage J, Henry M, Sanchez C (1988) Sol-Gel Chemistry of Transition-Metal Oxides. *Prog Solid State Chem* 18(4):259–341
39. Shimizu Y, Murata T (1997) Sol-gel synthesis of perovskite-type lanthanum manganite thin films and fine powders using metal acetylacetonate and poly(vinyl alcohol). *J Am Ceram Soc* 80(10):2702–2704
40. Zhou W, Ran R, Shao ZP, Jin WQ, Xu NP (2010) Synthesis of nano-particle and highly porous conducting perovskites from simple in situ sol-gel derived carbon templating process. *Bull Mat Sci* 33(4):371–376
41. Suciu C, Hoffmann AC, Dorolti E, Tetea R (2008) NiO/YSZ nanoparticles obtained by new sol-gel route. *Chem Eng J* 140(1–3):586–592
42. Jiang SP, Chan SH (2004) A review of anode materials development in solid oxide fuel cells. *J Mater Sci* 39(14):4405–4439
43. Wilson JR, Kobsiriphat W, Mendoza R, Chen HY, Hiller JM, Miller DJ, Thornton K, Voorhees PW, Adler SB, Barnett SA (2006) Three-dimensional reconstruction of a solid-oxide fuel-cell anode. *Nat Mater* 5(7):541–544
44. Wilkenhoener R, Vassen R, Buchkremer HP, Stover D (1999) Mechanically alloyed Ni/8YSZ powder mixtures: preparation, powder characterization and sintering behavior. *J Mat Sci* 34(2):257–265
45. Sun CW, Stimming U (2007) Recent anode advances in solid oxide fuel cells. *J Power Sources* 171(2):247–260
46. Jacobson AJ (2010) Materials for solid oxide fuel cells. *Chem Mat* 22(3):660–674
47. Tao SW, Irvine JTS (2003) A redox-stable efficient anode for solid-oxide fuel cells. *Nat Mater* 2(5):320–323
48. Wan J, Zhu JH, Goodenough JB (2006)  $\text{La}_{0.75}\text{Sr}_{0.25}\text{Cr}_{0.5}\text{Mn}_{0.5}\text{O}_{3-\delta} + \text{Cu}$  composite anode running on  $\text{H}_2$  and  $\text{CH}_4$  fuels. *Solid State Ion* 177(13–14):1211–1217

49. Zhu XB, Zhe L, Bo W, Chen KF, Liu ML, Huang XQ, Su WH (2010) Fabrication and performance of membrane solid oxide fuel cells with  $\text{La}_{0.75}\text{Sr}_{0.25}\text{Cr}_{0.5}\text{Mn}_{0.5}\text{O}_{3-\delta}$  impregnated anodes. *J Power Sources* 195(7):1793–1798
50. Fu XZ, Melnik J, Low QX, Luo JL, Chuang KT, Sanger AR, Yang QM (2010) Surface modified Ni foam as current collector for syngas solid oxide fuel cells with perovskite anode catalyst. *Int J Hydrogen Energy* 35(20):11180–11187
51. Chen XJ, Liu QL, Chan SH, Brandon NP, Khor KA (2007) Sulfur tolerance and hydrocarbon stability of  $\text{La}_{0.75}\text{Sr}_{0.25}\text{Cr}_{0.5}\text{Mn}_{0.5}\text{O}_3/\text{Gd}_{0.2}\text{Ce}_{0.8}\text{O}_{1.9}$  composite anode under anodic polarization. *J Electrochem Soc* 154(11):B1206–B1210
52. Ghouse M, Al-Musa A, Al-Yousef Y, Al-Otaibi MF (2010) Synthesis of Mg doped  $\text{LaCrO}_3$  nano powders by sol-gel process for solid oxide fuel cell (SOFC) application. *J New Mater Electrochem Syst* 13(2):99–106
53. Stover D, Buchkremer HP, Uhlenbruck S (2004) Processing and properties of the ceramic conductive multilayer device solid oxide fuel cell (SOFC). *Ceram Int* 30(7):1107–1113
54. Kueper TW, Visco SJ, De Jonghe LC (1992) Thin-film ceramic electrolytes deposited on porous and non-porous substrates by sol-gel techniques. *Solid State Ion* 52(1–3):251–259
55. Van Gestel T, Sebold D, Meulenber WA, Buchkremer H-P (2008) Development of thin-film nano-structured electrolyte layers for application in anode-supported solid oxide fuel cells. *Solid State Ion* 179(11–12):428–437
56. Pan Y, Zhu JH, Hu MZ, Payzant EA (2005) Processing of YSZ thin films on dense and porous substrates. *Surf Coat Technol* 200(5–6):1242–1247
57. Peshev P, Slavova V (1992) Preparation of Yttria-stabilized Zirconia thin-films by a sol-gel procedure using alkoxide precursors. *Mat Res Bull* 27(11):1269–1275
58. Gaudon M, Laberty-Robert C, Ansart F, Stevens P (2006) Thick YSZ films prepared via a modified sol-gel route: thickness control (8–80  $\mu\text{m}$ ). *J Eur Ceram Soc* 26(15):3153–3160
59. Egger P, Soraru GD, Dire S (2004) Sol-gel synthesis of polymer-YSZ hybrid materials for SOFC technology. *J Eur Ceram Soc* 24(6):1371–1374
60. Lenormand P, Rieu M, Cienfuegos RF, Julbe A, Castillo S, Ansart F (2008) Potentialities of the sol-gel route to develop cathode and electrolyte thick layers Application to SOFC systems. *Surf Coat Technol* 203(5–7):901–904
61. Vo NXP, Yoon SP, Nam SW, Han J, Lim TH, Hong SA (2005) Fabrication of an anode-supported SOFC with a sol-gel coating method for a mixed-gas fuel cell. On the Convergence of Bio-Information-, Environmental-, Energy- Space- and Nano-Technologies, Pts 1 and 2, 277(–279):455–461
62. Chen YY, Wei WCJ (2006) Processing and characterization of ultra-thin yttria-stabilized zirconia (YSZ) electrolytic films for SOFC. *Solid State Ion* 177(3–4):351–357
63. Agarwal V, Liu ML (1997) Preparation of barium cerate-based thin films using a modified Pechini process. *J Mater Sci* 32(3):619–625
64. Chiba R, Yoshimura F, Yamaki J, Ishii T, Yonezawa T, Endou K (1997) Ionic conductivity and morphology in  $\text{Sc}_2\text{O}_3$  and  $\text{Al}_2\text{O}_3$  doped  $\text{ZrO}_2$  films prepared by the sol-gel method. *Solid State Ion* 104(3–4):259–266
65. Mehta K, Xu R, Virkar AV (1998) Two-layer fuel cell electrolyte structure by sol-gel processing. *J Sol-Gel Sci Technol* 11(2):203–207
66. Jang WS, Hyun SH, Kim SG (2002) Preparation of YSZ/YDC and YSZ/GDC composite electrolytes by the tape casting and sol-gel dip-drawing coating method for low-temperature SOFC. *J Mater Sci* 37(12):2535–2541
67. Kim SG, Yoon SP, Nam SW, Hyun SH, Hong SA (2002) Fabrication and characterization of a YSZ/YDC composite electrolyte by a sol-gel coating method. *J Power Sources* 110(1):222–228
68. Rose L, Kesler O, Tang ZL, Burgess A (2007) Application of sol gel spin coated yttria-stabilized zirconia layers for the improvement of solid oxide fuel cell electrolytes produced by atmospheric plasma spraying. *J Power Sources* 167(2):340–348

69. Kim SD, Hyun SH, Moon J, Kim JH, Song RH (2005) Fabrication and characterization of anode-supported electrolyte thin films for intermediate temperature solid oxide fuel cells. *J Power Sources* 139(1–2):67–72
70. Moon J, Song HS, Kim WH, Hyun SH, Kim J, Lee HW (2007) Effect of starting particulate materials on microstructure and cathodic performance of nanoporous LSM-YSZ composite cathodes. *J Power Sources* 167(2):258–264
71. Xia CR, Zhang YL, Liu ML (2003) LSM-GDC composite cathodes derived from a sol-gel process - Effect of microstructure on interfacial polarization resistance. *Electrochem Solid State Lett* 6(12):A290–A292
72. Zha SW, Zhang YL, Liu ML (2005) Functionally graded cathodes fabricated by sol-gel/slurry coating for honeycomb SOFCs. *Solid State Ion* 176(1–2):25–31
73. Tang ZL, Xie YS, Hawthorne H, Ghosh D (2006) Sol-gel processing of  $\text{Sr}_{0.5}\text{Sm}_{0.5}\text{CoO}_3$  film. *J Power Sources* 157(1):385–388
74. Yoon SP, Han J, Nam SW, Lim TH, Oh IH, Hong SA, Yoo YS, Lim HC (2002) Performance of anode-supported solid oxide fuel cell with  $\text{La}_{0.85}\text{Sr}_{0.15}\text{MnO}_3$  cathode modified by sol-gel coating technique. *J Power Sources* 106(1–2):160–166
75. Sholklapper TZ, Lu C, Jacobson CP, Visco SJ, De Jonghe LC (2006) LSM-infiltrated solid oxide fuel cell cathodes. *Electrochem Solid State Lett* 9(8):A376–A378
76. Zhang Q, Martin BE, Petric A (2008) Solid oxide fuel cell composite cathodes prepared by infiltration of copper manganese spinel into porous yttria stabilized zirconia. *J Mat Chem* 18(36):4341–4346
77. Matus YB, De Jonghe LC, Jacobson CP, Visco SJ (2005) Metal-supported solid oxide fuel cell membranes for rapid thermal cycling. *Solid State Ion* 176(5–6):443–449
78. Tucker MC (2010) Progress in metal-supported solid oxide fuel cells: A review. *J Power Sources* 195(15):4570–4582
79. Rieu M, Lenormand P, Panteix PJ, Ansart F (2008) New route to prepare anodic coatings on dense and porous metallic supports for SOFC application. *Fuel Cells Bull* 2008(12): 12–15
80. Rieu M, Lenormand P, Ansart F, Mauvy F, Fullenwarth J, Zahid M (2008) Preparation of Ni-YSZ thin and thick films on metallic interconnects as cell supports. Applications as anode for SOFC. *J Sol-Gel Sci Technol* 45(3):307–313
81. Marrero-Lopez D, Ruiz-Morales JC, Pena-Martinez J, Canales-Vazquez J, Nunez P (2008) Preparation of thin layer materials with macroporous microstructure for SOFC applications. *J Solid State Chem* 181(4):685–692
82. Jiang SP (2002) A comparison of O-2 reduction reactions on porous (La, Sr) $\text{MnO}_3$  and (La, Sr)(Co, Fe) $\text{O}_{3-\delta}$  electrodes. *Solid State Ion* 146(1–2):1–22
83. Murray EP, Sever MJ, Barnett SA (2002) Electrochemical performance of (La, Sr)(Co, Fe) $\text{O}_{3-\delta}$ -(Ce, Gd) $\text{O}_{3-\delta}$  composite cathodes. *Solid State Ion* 148(1–2):27–34
84. Yang L, Liu Z, Wang SZ, Choi YM, Zuo CD, Liu ML (2010) A mixed proton, oxygen ion, and electron conducting cathode for SOFCs based on oxide proton conductors. *Journal of Power Sources* 195(2):471–474
85. Lane JA, Benson SJ, Waller D, Kilner JA (1999) Oxygen transport in  $\text{La}_{0.6}\text{Sr}_{0.4}\text{Co}_{0.2}\text{Fe}_{0.8}\text{O}_{3-\delta}$  -delta. *Solid State Ion* 121(1–4):201–208
86. Prestat M, Koenig JF, Gauckler LJ (2007) Oxygen reduction at thin dense  $\text{La}_{0.52}\text{Sr}_{0.48}\text{Co}_{0.18}\text{Fe}_{0.82}\text{O}_{3-\delta}$  -delta electrodes. Part I: Reaction model and faradaic impedance. *J Electroceram* 18(1–2):87–101
87. Lee JW, Liu Z, Yang L, Abernathy H, Choi SH, Kim HE, Liu ML (2009) Preparation of dense and uniform  $\text{La}_{0.6}\text{Sr}_{0.4}\text{Co}_{0.2}\text{Fe}_{0.8}\text{O}_{3-\delta}$  -delta (LSCF) films for fundamental studies of SOFC cathodes. *J Power Sources* 190(2):307–310
88. Simner SP, Anderson MD, Engelhard MH, Stevenson JW (2006) Degradation mechanisms of La-Sr-Co-Fe- $\text{O}_3$ SOFC cathodes. *Electrochem Solid State Lett* 9(10):A478–A481
89. Kim JY, Sprenkle VL, Canfield NL, Meinhardt KD, Chick LA (2006) Effects of chrome contamination on the performance of  $\text{La}_{0.6}\text{Sr}_{0.4}\text{Co}_{0.2}\text{Fe}_{0.8}\text{O}_{3-\delta}$  cathode used in solid oxide fuel cells. *J Electrochem Soc* 153(5):A880–A886

90. Benson SJ, Waller D, Kilner JA (1999) Degradation of  $\text{La}_{0.6}\text{Sr}_{0.4}\text{Fe}_{0.8}\text{Co}_{0.2}\text{O}_{3-\delta}$  in carbon dioxide and water atmospheres. *J Electrochem Soc* 146(4):1305–1309
91. Liu M, Liu Z, Liu MF, Nie LF, Mebane DS, Wilson DS, Surdoyal W (2010) Solid oxide fuel cells having porous cathodes infiltrated with oxygen-reducing catalysts, US Patent Application No. 12/837,757
92. Lynch ME, Yang L, Qin W, Choi J-J, Liu M, Blinn K, Liu M (2011) Enhancement of  $\text{La}_{0.6}\text{Sr}_{0.4}\text{Co}_{0.2}\text{Fe}_{0.8}\text{O}_{3-\delta}$  durability and surface electrocatalytic activity by  $\text{La}_{0.85}\text{Sr}_{0.15}\text{MnO}_{3\pm\delta}$  investigated using a new test electrode platform. *Energy Environ Sci* 4(6):2249
93. Lou XY, Wang SZ, Liu Z, Yang L, Liu ML (2009) Improving  $\text{La}_{0.6}\text{Sr}_{0.4}\text{Co}_{0.2}\text{Fe}_{0.8}\text{O}_{3-\delta}$  cathode performance by infiltration of a  $\text{Sm}_{0.5}\text{Sr}_{0.5}\text{CoO}_{3-\delta}$  coating. *Solid State Ion* 180(23–25):1285–1289
94. Nie LF, Liu MF, Zhang YJ, Liu ML (2010)  $\text{La}_{0.6}\text{Sr}_{0.4}\text{Co}_{0.2}\text{Fe}_{0.8}\text{O}_{3-\delta}$  cathodes infiltrated with samarium-doped cerium oxide for solid oxide fuel cells. *J Power Sources* 195(15):4704–4708
95. Choi J-J, Qin W, Liu M, Liu M (2011) Preparation and characterization of  $(\text{La}_{0.8}\text{Sr}_{0.2})_{0.95}\text{MnO}_{3-\delta}$  (LSM) thin films and LSM/LSCF interface for solid oxide fuel cells. *J Am Ceram Soc* 94(10):3340–3345
96. Singhal SC (2000) Advances in solid oxide fuel cell technology. *Solid State Ion* 135(1–4):305–313
97. Gong MY, Liu XB, Tremblay J, Johnson C (2007) Sulfur-tolerant anode materials for solid oxide fuel cell application. *J Power Sources* 168(2):289–298
98. Atkinson A, Barnett S, Gorte RJ, Irvine JTS, Mcevoy AJ, Mogensen M, Singhal SC, Vohs J (2004) Advanced anodes for high-temperature fuel cells. *Nat Mater* 3(1):17–27
99. Park SD, Vohs JM, Gorte RJ (2000) Direct oxidation of hydrocarbons in a solid-oxide fuel cell. *Nature* 404(6775):265–267
100. Gorte RJ, Vohs JM (2003) Novel SOFC anodes for the direct electrochemical oxidation of hydrocarbons. *J Catal* 216(1–2):477–486
101. Lu C, Worrell WL, Gorte RJ, Vohs JM (2003) SOFCs for direct oxidation of hydrocarbon fuels with samaria-doped ceria electrolyte. *J Electrochem Soc* 150(3):A354–A358
102. Huang YH, Dass RI, Xing ZL, Goodenough JB (2006) Double perovskites as anode materials for solid-oxide fuel cells. *Science* 312(5771):254–257
103. Pillai MR, Kim I, Bierschenk DM, Barnett SA (2008) Fuel-flexible operation of a solid oxide fuel cell with  $\text{Sr}_{0.8}\text{La}_{0.2}\text{TiO}_3$  support. *J Power Sources* 185(2):1086–1093
104. Pillai MR, Jiang Y, Mansourian N, Kim I, Bierschenk DM, Zhu HY, Kee RJ, Barnett SA (2008) Solid oxide fuel cell with oxide anode-side support. *Electrochem Solid State Lett* 11(10):B174–B177
105. Fu QX, Tietz F, Stover D (2006)  $\text{La}_{0.4}\text{Sr}_{0.6}\text{Ti}_{1-x}\text{Mn}_x\text{O}_{3-\delta}$  perovskites as anode materials for solid oxide fuel cells. *J Electrochem Soc* 153(4):D74–D83
106. Yoon SP, Han J, Nam SW, Lim TH, Hong SA (2004) Improvement of anode performance by surface modification for solid oxide fuel cell running on hydrocarbon fuel. *J Power Sources* 136(1):30–36
107. Zhu JH, Zhang Y, Basu A, Lu ZG, Paranthaman M, Lee DF, Payzant EA (2004)  $\text{LaCrO}_3$ -based coatings on ferritic stainless steel for solid oxide fuel cell interconnect applications. *Surf Coat Technol* 177:65–72
108. Pu JA, Hua B, Zhang WY, Wu JA, Chi B, Jian L (2010) A promising  $\text{NiCo}_2\text{O}_4$  protective coating for metallic interconnects of solid oxide fuel cells. *J Power Sources* 195(21):7375–7379
109. Fang Y, Wu C, Duan X, Wang S, Chen Y (2011) High-temperature oxidation process analysis of  $\text{MnCo}_2\text{O}_4$  coating on Fe–21Cr alloy. *Int J Hydrogen Energy* 36(9):5611–5616
110. Hua B, Kong YH, Lu FS, Zhang JF, Pu JA, Li JA (2010) The electrical property of  $\text{MnCo}_2\text{O}_4$  and its application for SUS 430 metallic interconnect. *Chin Sci Bull* 55(33):3831–3837

Sol-Gel Processing for Conventional and Alternative  
Energy

Aparicio, M.; Jitianu, A.; Klein, L.C. (Eds.)

2012, X, 397 p., Hardcover

ISBN: 978-1-4614-1956-3